Available online at www.sciencedirect.com

ScienceDirect

Developmental Biology 303 (2007) 825–837

DEVELOPMENTAL BIOLOGY

www.elsevier.com/locate/ydbio

Genomes & Developmental Control

Dosage-dependent transcriptional regulation by the calcineurin/NFAT signaling in developing myocardium transition

Xiao Yong Yang [a], Teddy T.C. Yang [a], William Schubert [a], Stephen M. Factor [b], Chi-Wing Chow [a,*]

[a] *Department of Molecular Pharmacology, Albert Einstein College of Medicine, Jack and Pearl Resnick Campus, 1300 Morris Park Ave, Bronx, NY 10461, USA*
[b] *Department of Pathology and Medicine, Albert Einstein College of Medicine, Jack and Pearl Resnick Campus, Bronx, NY 10461, USA*

Received for publication 9 August 2006; revised 9 November 2006; accepted 22 November 2006
Available online 2 December 2006

Abstract

Thin spongy myocardium is critical at early embryonic stage [before embryonic day (E) 13.5 in mice] to allow diffusion of oxygen and nutrients to the developing cardiomyocytes. However, establishment of compact myocardium at later stage (~E16.5) during development is necessary to prepare for the increase in demand for blood circulation. Elucidating molecular targets of the spongy–compact myocardium transition between E13.5 and E16.5 in heart development is thus important. Previous studies demonstrated that multiple transcription factors and signaling pathways are involved in the regulation and function of the myocardium in heart development. Disruption of certain transcription factors or critical components of signaling pathways frequently causes structural malformation in heart and persistence of "thin spongy myocardium". We have recently demonstrated activation of the calcineurin/NFAT signaling pathway at E14.5 in developing myocardium. Constitutive inhibition of the calcineurin/NFAT signaling pathway caused embryonic lethality. Molecular targets downstream of the calcineurin/NFAT signaling pathway, however, remains elusive. Here, we report transcription targets, independently and dependently, regulated by the calcineurin/NFAT signaling during the E13.5–E16.5 myocardium transition. We have uncovered that expression of one-third of the induced genes during myocardium transition is calcineurin/NFAT-dependent. Among these calcineurin/NFAT-dependent transcription targets, there is a dosage-dependent regulation. Molecular studies indicate that formation of distinct NFAT:DNA complex, in part, accounts for the dosage-dependent regulation. Thus, in addition to temporal and spatial regulation, dosage-dependent threshold requirement provides another mechanism to modulate transcription response mediated by the calcineurin/NFAT signaling during heart development.

Keywords: Heart development; Myocardium transition; Transcription regulation; Calcineurin signaling; Transcription factor NFAT

Introduction

Heart is the first organ to form during gestation (Kaufman, 1992; Kaufman and Bard, 1999). Multiple transcription factors and signaling pathways are involved in the regulation and function of the myocardium in heart development (Bruneau, 2002; Harvey and Rosenthal, 1999; MacLellan and Schneider, 2000; Srivastava, 2001; Srivastava and Olson, 2000). This process involves proliferation and differentiation of cardiomyocytes, which are regulated in a synchronized and temporal manner. Many of these signaling pathways are also activated to compensate for diminished cardiac output and to increase workload of diseased hearts. Thus, understanding the molecular basis of heart development will shed new light on congenital heart defects as well as adult heart disease.

Previous gene targeting studies have demonstrated that disruption of certain transcription factors or critical components of signaling pathways frequently causes structural malformation in heart and persistence of "thin spongy myocardium", which results in congenital heart defects and causes premature death. Formation of thin spongy myocardium is critical at early embryonic stage [before embryonic day (E) 13.5 in mice] to allow diffusion of oxygen and nutrients to the developing cardiomyocytes. However, establishment of compact myocardium at later stage (~E16.5) during development is necessary to substitute the spongy myocardium to prepare for the increase in demand for blood circulation. The underlying molecular

* Corresponding author. Fax: +1 718 430 8922.
E-mail address: cchow@aecom.yu.edu (C.-W. Chow).

0012-1606/$ - see front matter © 2006 Elsevier Inc. All rights reserved.
doi:10.1016/j.ydbio.2006.11.036

mechanism of the spongy–compact myocardium transition at E13.5–E16.5 in heart development, however, has yet to be established.

The vertebrate specific calcineurin/transcription factor NFAT signaling pathway regulates gene expression in immune and non-immune cells (Crabtree and Olson, 2002; Hogan et al., 2003; Horsley and Pavlath, 2002; Macian, 2005). Previous studies showed that targeted disruption of NFATc1 impairs heart valve and septum formation and hence causes embryonic lethality by E14.5 (de la Pompa et al., 1998; Ranger et al., 1998). Recent studies further demonstrated a field of endocardium–myocardium interaction is necessary for the induction of heart valves (Chang et al., 2004). Specifically, repression of NFAT target – VEGF – provides an instructive role for heart valve formation.

In addition to heart valve formation, NFATc3 and NFATc4 are required for vasculature development in heart between E7.5 and E8.5 (Bushdid et al., 2003; Graef et al., 2001). Combined disruption of NFATc3 and NFATc4 causes embryonic lethality. The requirement of two NFAT members in vasculature formation implicates a possible functional redundancy and/or threshold regulation in the calcineurin/NFAT signaling pathway.

The calcineurin/NFAT signaling also plays a key role in cardiac hypertrophy in adult heart (Molkentin et al., 1998). Cardiac hypertrophy is frequently associated with reactivation of fetal genes involved in heart development in the myocardium (Frey and Olson, 2003; Molkentin and Dorn, 2001; Petrich and Wang, 2004). Together, these studies elucidate distinct roles (spatially and temporally) of NFAT in heart development and disease. However, targets of the calcineurin/NFAT signaling pathway in cardiac myocytes, which are maturated at later stages during development, remain elusive.

Recently, we have established transgenic mice expressing dominant-negative NFAT inhibitor (dnNFAT) in heart (Schubert et al., 2003). Since constitutive expression of the dnNFAT in myocardium causes embryonic lethality, we have conditionally expressed the dnNFAT in heart. We have demonstrated NFAT activation during myocardium transition at E14.5. Inhibition of NFAT causes thin myocardium in the developing atria. Ultrastructural studies demonstrated disrupted sarcomere and molecular analysis demonstrated reduced expression of cardiac troponin-I and cardiac troponin-T at birth. Increased expression of dnNFAT causes more severe deformation in heart and the majority of transgenic embryos are found dead by E16.5 (data not shown). Although these studies further demonstrated the spatial and temporal requirement of the calcineurin/NFAT signaling, the transcription profile mediated by the calcineurin/NFAT signaling in the E13.5–E16.5 myocardium transition remains unknown.

The purpose of this study was to profile molecular targets and elucidate the contribution of calcineurin/NFAT signaling during E13.5–E16.5 myocardium transition. Here, we report transcription targets, independently and dependently, regulated by the calcineurin/NFAT signaling during the E13.5–E16.5 myocardium transition. We have uncovered that expression of one-third of the induced genes during E13.5–E16.5 myocardium transition requires calcineurin/NFAT activation. For the expression of the calcineurin/NFAT-dependent transcription targets, there is a dosage-dependent threshold regulation. Formation of distinct NFAT:DNA complex, in part, accounts for the dosage-dependent regulation. Thus, in addition to temporal and spatial regulation, threshold requirement provides another mechanism to modulate transcription response mediated by the calcineurin/NFAT signaling.

Materials and methods

Mice

Animal experiments were performed in accordance with guidelines of Albert Einstein College of Medicine Institute of Animal Studies. All mice were in C57BL/6 background. Timed-pregnant mice were injected subcutaneously with cyclosporin A daily at 40 mg/kg/day (low dose) and 80 mg/kg/day (high dose) starting at E13.5. Embryos were harvested on E16.5 and hearts were prepared.

Embryonic heart preparation

Embryonic hearts were harvested at various times during gestation as indicated. The date after conception was registered as embryonic day (E) 0.5. On the day of harvest, the embryos were decapitated and the remaining torso was fixed in 10% buffered formalin overnight before isolation of the hearts through a dissecting microscope. Isolated hearts were put in cassette and immersed in 70% alcohol before processed through a graded series of alcohols and xylene in an automated tissue processor. Isolated hearts were then immersed in paraffin, oriented and embedded. Embedded hearts were serially sectioned sagittally at a thickness of 7 μm using a Microm microtome (Baxter Scientific) and placed on super-frost plus slides (Fisher Scientific). Representative sections were hematoxylin and eosin-stained and examined under a microscope.

Microarray analysis

Microarray experiments were designed to profile gene expression during E13.5–E16.5 myocardium transition. Role of calcineurin/NFAT in myocardium transition was also investigated by subcutaneous injection of calcineurin inhibitor Cyclosporin A (CsA) into time-pregnant mice starting at E13.5. Pregnant mice were injected with two different doses of CsA (40 mg/kg/day or 80 mg/kg/day), and embryonic hearts were isolated at E16.5. An Affymetrix GeneChip Mouse Genome set 430 2.0 array consisting>45,000 probe sets, representing over 34,000 mouse genes, was used. Total RNA was isolated separately from hearts of E13.5, E16.5, (E16.5+low CsA) and (E16.5+high CsA) using Trizol reagents and purified by Rneasy Fibrous Tissue Mini Kit (Qiagen). Ten hearts from each condition were pulled together for RNA preparation. Total RNA (5 μg) of each sample was first reverse transcribed with T7-oligo (dT) promoter-primer in the first-strand cDNA synthesis using Superscript II reverse transcriptase. Then RNase H-mediated second strand cDNA was synthesized by DNA polymerase I. Double-stranded cDNA was purified and served as a template in the subsequent *in vitro* transcription reaction. Complementary RNA (cRNA) was synthesized and biotin labeled overnight in the presence of T7 RNA polymerase and biotinylated nucleotide analog/ribonucleotide mix. The biotinylated cRNA targets were then cleaned up, fragmented and hybridized to GeneChip expression arrays for 16 h. After washing and staining, the image was scanned and analyzed using Affymetrix Microarray Suit Software 5.0, which conducted normalization and scaling of the data. When two arrays were compared, the cRNA expression level of a transcript was directly proportional to the signal intensity, which was a quantitative value calculated for each probe. Signal log ratio estimated the magnitude of change between different arrays. Robust changes were identified by selecting transcripts with fold change>2 for increase and decrease targets, which corresponded to an absolute signal log ratio>1. Candidate genes were selected from all profiles (*i.e.* E13.5 *versus* E16.5, or E16.5 hearts:untreated *versus* CsA treated) with a difference of>2-fold. In addition, a changing *p*-value less than or equal to 0.05 must be satisfied, which represented a high probability of significant increase/decrease between arrays. Candidate genes were verified by RT-PCR based on

their EST expression profile in heart and in gestation stage using the NCBI UniGene database.

Gene cluster analysis was processed by TMEV (TIGR Multiple Experiment Viewer) software version 3.1. Signal intensities of the genes were log10 transformed, then imported into the TMEV software for Gene/Row adjustments. Gene cluster was generated using Euclidean metric with complete linkage. The image was colored to represent increase (red) or decrease (green) in intensity. Pathway analysis was performed by using pathway-express software of Onto-Tools from Wayne State University, a derivative of the Kyoto Encyclopedia of Genes and Genomes (KEGG) pathway database. This modified software allows construction of all associated signaling pathways based on the gene profile. Affymetrix probe IDs were input into the software and genes involved in possible signaling pathways were revealed and categorized (Table 1 and supplemental data Tables S2–S10).

Semi-quantitative RT-PCR

Total RNA was isolated from embryonic hearts using TRIZOL reagents (Invitrogen). Isolated RNA (1 μg) was reverse transcribed with Superscript II reverse transcriptase (Invitrogen), and cDNA prepared was amplified by PCR, separated and visualized by agarose gel electrophoresis. At least two amplifications with different cycles were performed. Intensity of PCR products from three independent experiments was quantified by ImageQuant 5.0 software (Adobe). Primers for PCR amplification were summarized in Table S1 in supplemental data.

Morphometric analysis

To determine ventricular wall thickness, digital images of embryonic hearts were generated. Images were selected based on their similar morphological appearances containing all four chambers and valves. Using the generated images, equal distance was extended from the apex to the top of the left and right ventricles along the circumference of the heart. A total of eight different locations were marked. Thickness of each location along the ventricular walls was measured from 10 images. The averages were then graphed and presented.

Gel mobility shift assays

Nuclear extracts were prepared from cells transfected with NFAT expression vector as described previously (Yang and Chow, 2003; Yang et al., 2002). In brief, double-stranded oligonucleotides (100 fmol) were labeled with [α-^{32}P] dCTP using DNA polymerase I Klenow fragments. Binding reactions for gel mobility shift assays were carried out at RT in gel-shift buffer [1 mM $CaCl_2$, 1 mM $MgCl_2$, 10 mM Hepes (pH 7.9), 50 mM NaCl, 15 mM β-mercaptoethanol, 10% glycerol, 0.1 mg/ml bovine serum albumin, and 1 mg/ml poly dI:dC] for 30 min. Protein:DNA complexes were separated in 5% non-denaturing polyacrylamide gels in Tris–glycine–EDTA buffer [25 mM Tris, 200 mM glycine, and 1 mM EDTA] and visualized by autoradiography. For supershift analysis, antibody was pre-incubated with nuclear extract for 30 min at RT before addition of the labeled probe. For competition analysis, excess amount of unlabeled IL-2 NFAT oligonucleotides (5000 fmol, or 500, 1000, and 2500 fmol of different competitors for cross-competition analysis) were incubated together with the labeled probe before addition of the nuclear extract. To determine the relative binding of the NFAT:DNA complex, saturation analysis was performed. In brief, increasing amount of labeled probe (50, 100, and 150 fmol) was incubated with constant amount of nuclear extract. The amount of NFAT:DNA complexes and unbound probe were quantitated by PhosphoImager analysis. The ratio of bound/free was plotted against the amount of bound and presented. Sequence for the NFAT sites of the Agtr2 and Reg3γ promoter is (Agtr2: −701 bp 5′-CAG-AGAAAAGGAAAAACAGTCATAACCATA-3′; −1951 bp 5′-GTTTCCTAGACATCA-GGTTTCCATTATTTA-3′; −5251 bp 5′-GTATTT-GTGGCAAGTTTTCCCAGACTGTAT-3′; Reg3γ: −201 bp 5′-ATAG-TATCTGGGAAAA-GATGGGGAAAGTTC-3′; −251 bp 5′-TATGTTCCG-GAAAACTTATAGAAATAATAG-3′). Sequence for the interleukin-2 ARRE NFAT is (5′-AGAAAGGAGGAAAAACTGTTTCATA-CAGAAGG-3′).

Table 1
Transcription targets elicited upon myocardium transition modulate various signaling pathways

Signaling pathways	Regulated by		Target genes
	E13.5 vs E16.5	Calcineurin/NFAT	
Calcium signaling pathway	+	−	Cacna1g, Ryr2, Prkcb1, Mylk, Adcy9, Atp2a3, Tnnt1, Casq2, Fhl2
	+	++	Tnnc2, Lck, Camk4, Ptprc, Myh3
	+	+	Cckar, Myh8, Fkbp5
Wnt signaling pathway	+	−	Myc, Wif1, Prkcb1, Wnt5a
	+	++	Rac2, Lef1
	+	+	Tcf7
Notch signaling pathway	+	−	Dtx1
	+	++	Ptcra
	+	+	
Ligand–receptor interaction	+	−	Lepr, P2rx1, Agtr, Rgs5, Oprl1
	+	++	Pery10, Gzma
	+	+	Agtr2, Cckar, Gpr64, Angptl1, C1qtnf3, Reg3g
Tight junction	+	−	Cldn5, Cldn7, Cldn8, Crb3, Prkcb1, Hcls1
	+	++	Cldn18
	+	+	Cldn3, Cldn10
Focal adhesion	+	−	Vav1, Vtn, Parvg, Col1a1, ltga7, Cav1, Cav2, App1, Mylk, Flnb4
	+	++	Coro1a, Eva1, Pscdbp
	+	+	Col11a1
Adherens junction	+	−	
	+	++	Cdh1, Lef1, Hcph, Rac2
	+	+	Tcf7
Cytokine–cytokine receptor interaction	+	−	lL1f2, Amhr2, Tnfsf11, Tslp, Lepr
	+	++	lL7, Ccl25, Cxcl10, lL2ra, Ltb, Cxcl15, Ccr9
	+	+	Cxcl13, Gdf10
Complement and coagulation cascades	+	−	C1S, F13a1, C3
	+	++	
	+	+	F3, Anxa8

Results

Dosage–responsive reduction of myocardium walls upon NFAT inhibition by cyclosporin A

We have recently demonstrated that calcineurin/NFAT is required for the late morphogenesis (after E14.5) of heart maturation (Schubert et al., 2003). Inhibition of NFAT activity by conditional expression of a dominant negative inhibitor (dnNFAT) in heart leads to thin atrial myocardium and sarcomere disorganization. Increase expression of dnNFAT, however, causes more severe deformation in both chambers and the majority of transgenic embryos are found dead by E16.5 (data not shown). These data are corroborated by the observation that constitutive expression of the dnNFAT in myocardium caused embryonic lethality (data not shown). Together, these data indicate that the calcineurin/NFAT signaling pathway contributes significantly to the myocardium transition. Further elucidating the expression of downstream targets of the calcineurin/NFAT signaling pathway is important.

To circumvent the embryonic lethality of the dnNFAT transgenic mice, we utilized calcineurin inhibitor cyclosporin A (CsA) to block NFAT activation *in vivo*. CsA blocks calcineurin activation and thus, impedes subsequent NFAT nuclear localization and function. We administered CsA subcutaneously to time-pregnant C57BL/6 mice from E13.5 to E16.5 to block calcineurin activation during myocardium transition. Injection of CsA starting at E13.5 will thus bypass the inhibition on vasculature formation and heart valve differentiation. Two different doses of CsA (low, 40 mg/kg/day; high, 80 mg/kg/day) were administered, in the range of CsA used in previous studies (Bueno et al., 2002; Gafter-Gvili et al., 2003; Zhang, 2002), to ascertain efficacy of delivery to developing embryos and to allow full extent of calcineurin inhibition.

We performed histological analysis on E16.5 hearts of C57BL/6 mice given or not CsA starting on E13.5. Histological analysis of E16.5, CsA-treated hearts revealed thinning in their atrial and ventricular myocardium as compared to untreated hearts (Fig. 1A). Importantly, a dosage-dependent reduction of the myocardium thickness was observed upon CsA administration. Morphometric analysis of the myocardium thickness revealed a graded reduction of the ventricular walls upon CsA administration (Fig. 1B). These data indicate that a dosage-dependent threshold regulation of the calcineurin/NFAT signaling pathway by CsA inhibition leads to a gradual thinning in the developing myocardium. In addition, these data support that heightened NFAT inhibition leads to more severe heart deformation and embryonic lethality.

Transcription profile during myocardium transition

Next, we investigated the molecular targets mediated by the calcineurin/NFAT signaling during myocardium transition. To profile the molecular targets during myocardium transition, we performed microarray analysis to determine gene expression in hearts isolated from E13.5 and E16.5 embryos. Differentially expressed targets found at these stages would likely play a critical role in myocardium transition. In addition, RNA isolated from E16.5, cyclosporin A (CsA)-treated hearts were also subjected to microarray analysis to elucidate the contribution of calcineurin/NFAT signaling in myocardium transition.

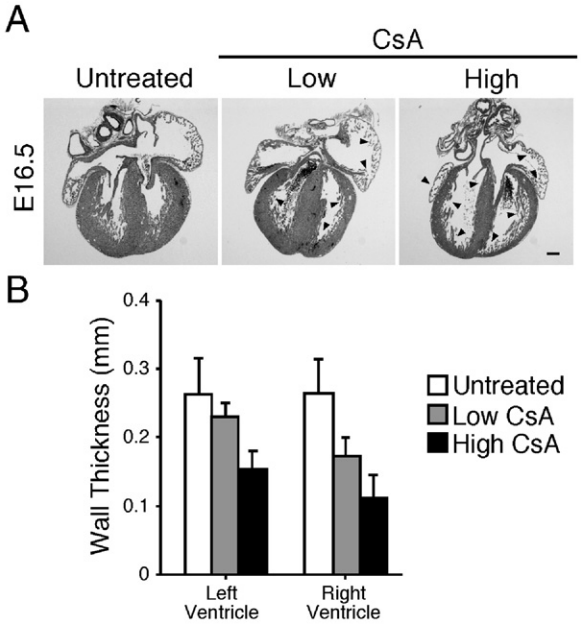

Fig. 1. Dosage–responsive reduction of E16.5 myocardium walls upon NFAT inhibition by cyclosporin A. Timed-pregnant mice were given low and high dosage of cyclosporin A (CsA). Hearts isolated from untreated and CsA-treated embryos were fixed in 10% formalin, processed, embedded, and serial sectioned sagittally. Representative sections, from at least 10 embryos in two different litters, were shown (panel A). Cross-sectional thickness of ventricular walls, from 10 different embryos, were measured (panel B). Scale bar=200 μm. *$p \leq 0.05$; †$p \leq 0.005$.

Four transcription profiles were analyzed: E13.5, E16.5, and E16.5 treated with low or high dosage of CsA. Transcription profile from E13.5 heart was cross compared with transcription profile from E16.5 heart (E16.5 *versus* E13.5) to identify developmentally regulated genes that might play a role in myocardium transition. Similarly, transcription profile from untreated E16.5 hearts was cross compared with transcription profile from E16.5 hearts treated with low or high dosage of CsA, [(E16.5: untreated *versus* low CsA) and (E16.5: untreated *versus* high CsA)], to identify calcineurin-regulated genes. Data mining analysis was further performed by contrasting of the transcription profiles between (E16.5 *versus* E13.5) and (E16.5: untreated *versus* low CsA) or (E16.5: untreated *versus* high CsA) to identify developmental transcription targets that are calcineurin/NFAT-dependent during myocardium transition (Fig. 2, also in supplemental data Figs. S1–S4).

With a filter for fold changes >2, our microarray analysis demonstrated that expression of 878 genes were increased and 260 genes were decreased during E13.5–E16.5 myocardium transition (Figs. 2 and 3). Upon CsA inhibition, 388 genes were increased and 277 genes were decreased in E16.5 hearts. Among all the differential expressed genes during E13.5–E16.5 myocardium transition, 278 of increased genes and 13 of decreased genes were sensitive to CsA inhibition. Hence, about one-third of increased genes (278/878) during myocardium

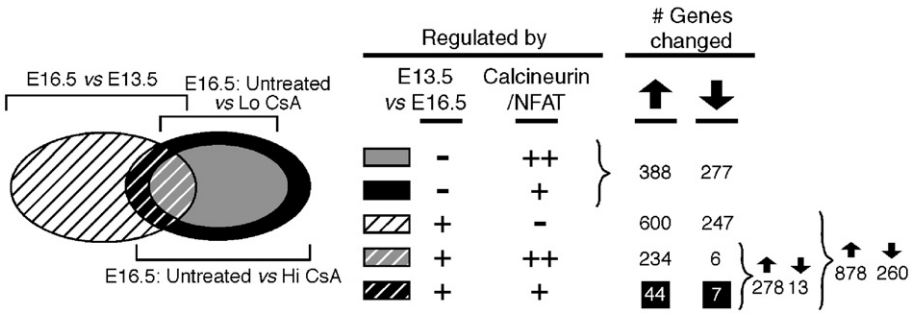

Fig. 2. Transcription profile during myocardium transition. Schematic representation of microarray analysis. Total RNA isolated from embryonic day (E) 13.5, E16.5, and E13.5–E16.5 cyclosporin A (CsA)-treated hearts [low (Lo) and high (Hi) dosage] were reverse transcribed, labeled, and hybridized to Affymetrix 430 2.0 array DNA chips. Transcription profiles of myocardium transition from E13.5 to E16.5 (E13.5 *versus* E16.5), and untreated E16.5 heart *versus* CsA treated E16.5 heart (E16.5: Untreated *versus* Lo CsA and E16.5: Untreated *versus* Hi CsA) were examined. Hatched boxes represent E13.5–E16.5 regulated genes. Shaded or filled boxes represent calcineurin/NFAT-regulated genes. Darker shade represents higher amount of CsA is required to regulate these transcription targets. Number of genes changed is also indicated and is represented by filled arrows (up, increased genes; down, decreased genes). Number of genes that are differentially regulated by high, but not low, dosage of CsA is highlighted.

transition were mediated by the calcineurin/NFAT signaling pathway. Conversely, the calcineurin/NFAT signaling only modestly regulated gene reduction (13/260) during myocardium transition. Expression of the remaining 600 increased genes and 247 decreased genes was independent of calcineurin/NFAT regulation during E13.5–E16.5 myocardium transition. Among the 278 calcineurin/NFAT increased and 13 decreased genes, expression of 44 increased genes and 7 decreased genes were inhibited only at high CsA concentration. Clustering analysis further demonstrated that these 44 differentially regulated genes (Fig. 3D) exhibited different induction profile as compared to the remaining 234 genes, which were sensitive to both high and low CsA concentration (Fig. 3B). Together, these data reveal transcription profiles, which are calcineurin/NFAT dependent and independent, during myocardium transition. In addition, there is a dosage-dependent threshold regulation for the transcription of some calcineurin/NFAT-dependent molecular targets.

Data mining analysis further indicated that transcription targets elicited upon myocardium transition could be classified into various signaling pathways. These included calcium signaling pathway, Wnt signal transduction, and many ligand–receptor interactions (Table 1). Notably, gene targets involved in cell–cell contact (*e.g.* tight junction and focal adhesion) were also modulated upon myocardium transition. Presumably, secure cell–cell contact is required to provide communication (*e.g.* calcium mobilization) as well as synchronized contraction in the mature myocardium upon stimulation.

Calcineurin/NFAT-independent transcription regulation during myocardium transition

To validate differential expression of the identified molecular targets during E13.5 and E16.5 myocardium transition, we performed RT-PCR analysis. We selected a handful of representative genes (Tables 2 and 3) based on i) EST expression profile in heart, ii) EST expression profile during gestation, and/or iii) potential function in heart. RT-PCR analysis demonstrated that increased expression of acyl-CoA synthetase long-chain family member 1 (Ascl1), calsequestrin 2 (Casq2), creatine kinase mitochondrial 2 (Ckmt2), cytochrome *c* oxidase subunit VIIa1 (Cox7a1), cytochrome *c* oxidase subunit VIIIb (Cox8b), fatty acid binding protein 4 (Fabp4), four and a half LIM domains 2 (Fhl2), myomesin 2 (Myom2), regulator of G-protein signaling 5 (Rgs5), and S100 calcium binding protein A1 (S00A1) (Figs. 4A and B), whereas expression of EGF-like repeats and discoidin I-like domain 3 (Edil3), heparin sulfate 6-*O*-sulfotransferase 2 (Hs6st2), opioid receptor-like 1 (Oprl1), slow skeletal troponin T1 (Tnnt1); and wingless-related MMTV integration site 5A (Wnt5a) were decreased (Figs. 4C and D) during E13.5–E16.5 myocardium transition. Transcription of all these differentially expressed genes, however, were calcineurin/NFAT-independent as their expression levels were similar in the presence and absence of CsA treatment. Expression of glyceraldehydes-3-phosphate dehydrogenase (Gapdh) and ribosomal protein L32 (Rpl32) were used as controls. These data support the microarray analysis for the differential expression of molecular targets.

Transcription targets regulated by the calcineurin/NFAT signaling during myocardium transition

We also performed RT-PCR to ascertain the differential regulation of molecular targets that were calcineurin/NFAT-dependent. RT-PCR analysis demonstrated that increased expression of angiotensin I converting enzyme 2 (Ace2), carboxylesterase 3 (Ces3), coronin, actin binding protein 1A (Coro1a), deltex 1 homolog (Dtx1), keratin complex 2, basic gene 8 (Krt2-8), lymphoid enhancer binding factor 1 (Lef1), NADPH dehydrogenase quinone 1 (Nqo1), secretoglobin family 1A, member 1 (Scgb1a1), secretoglobin family 3A, member 1 (Scgb3a1), transcription factor 7 (Tcf7), and transformation related protein 63 (Trp63) upon E13.5–E16.5 myocardium transition (Figs. 5A and B). Induction of these genes, however, was abrogated by low or high CsA inhibition. We also uncovered molecular targets that were calcineurin/NFAT-dependent, but independent of E13.5–E16.5 myocardium transition (Figs. 5C and D). Examples in this group of transcription targets were lymphocyte cytosolic protein 1 (Lcp1) and Ras association domain family 5 (Rassf5). Similar expression of Gapdh was used as control.

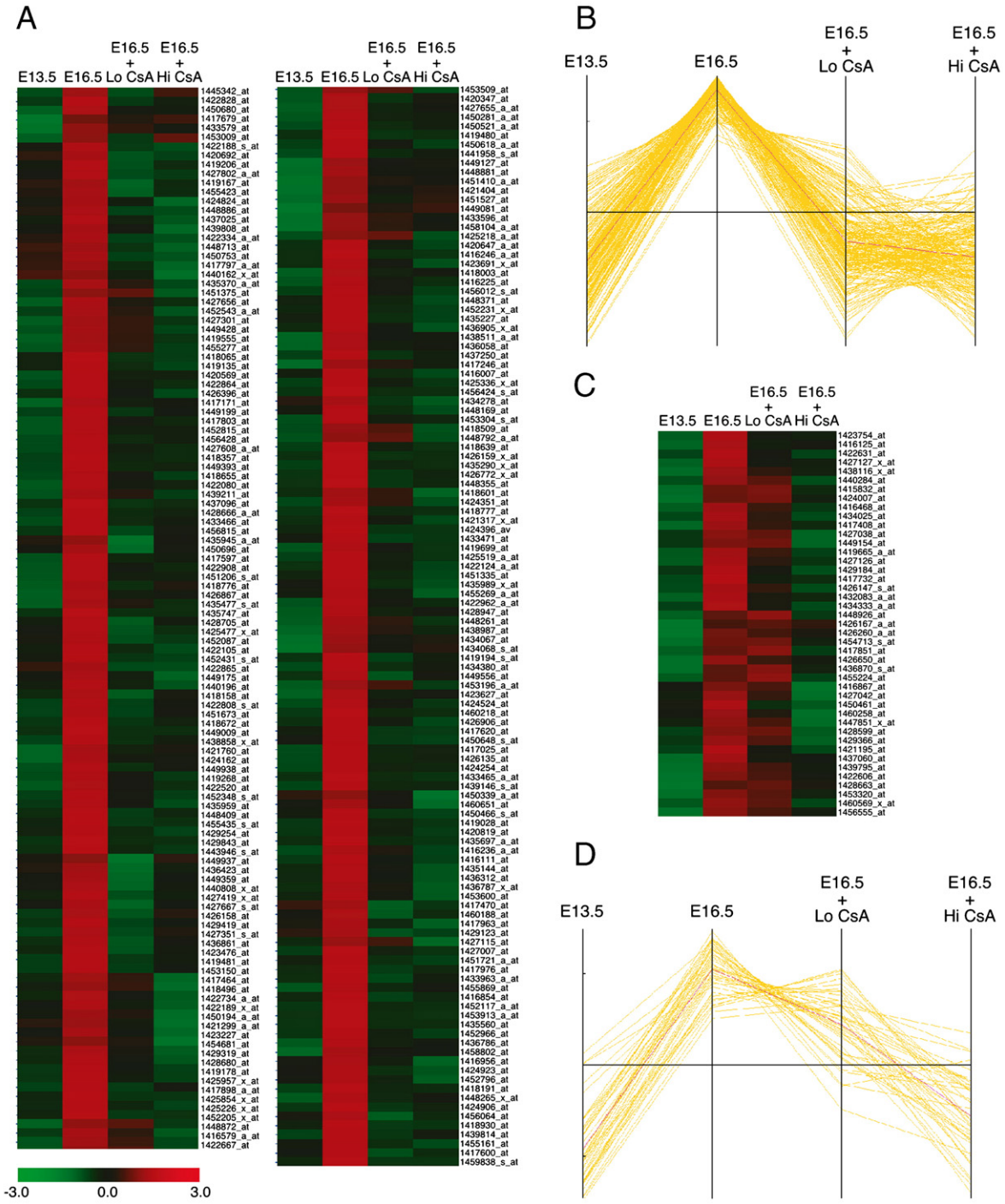

Fig. 3. Clustering analysis of genes regulated by the calcineurin/NFAT signaling during myocardium transition. A) Signal intensities of 234 increased genes that were CsA dependent from E13.5 to E16.5 were analyzed by TMEV (TIGR Multiple Experiment Viewer) and presented. Expression levels were colored coordinated with green for low intensity and red for high intensity. B) Expression pattern of the 234 increased genes indicated inhibition by CsA at low and high dosages. C) Signal intensities of 44 increased genes that were CsA threshold dependent were presented. D) Expression pattern of the 44 increased genes indicated that these genes were more sensitive to high dosage of CsA inhibition during E13.5–E16.5 myocardium transition.

Dosage-dependent threshold requirement on transcription targets regulated by the calcineurin/NFAT signaling during myocardium transition

Unexpectedly, increased expression of some calcineurin/NFAT-dependent targets during E13.5–E16.5 myocardium transition were blocked by CsA inhibition only at high, but not low, concentration (Fig. 6). These threshold-sensitive genes included angiotensin II receptor type 2 (Agtr2), carbonyl reductase 2 (Cbr2), cytochrome P450 family 2, subfamily f, polypeptide 2 (Cyp2f2), forkhead box A1 (Foxa1), regenerating islet-derived 3 gamma (Reg3γ), and SRY-box containing gene 2

Table 2
Transcription targets during myocardium transition—calcineurin/NFAT-independent

Gene title	Gene symbol	Fold Δ	Unigene ID
E13.5–E16.5 transition, CsA independent up-regulated genes			
Acyl-CoA synthetase long-chain family member 1	Ascl1	4.3 [a]	Mm.210323
Calsequestrin 2	Casq2	2.3	Mm.15343
Creatine kinase, mitochondrial 2	Ckmt2	7.0	Mm.316438
Cytochrome *c* oxidaase subunit VIIa1	Cox7a1	2.1	Mm.12907
Cytochrome *c* oxidaase subunit VIIIb	Cox8b	4.6	Mm.3841
Fatty acid binding protein 4	Fabp4	2.6	Mm.582
Four and a half LIM domains 2	Fhl2	2.1	Mm.6799
Myomesin 2	Myom2	9.2	Mm.272115
Regulator of G-protein signaling 5	Rgs5	2.6	Mm.20954
S100 calcium binding protein A1	S100A1	2.0	Mm.24662
E13.5–E16.5 transition, CsA independents down-regulated genes			
EGF-like repeats and discoidin I-like domain 3	Edil3	−2.8	Mm.125580
Herapin sulfate 6-0-sulfotransferase 2	Hs6st2	−2.3	Mm.252561
Opioid receptor-like 1	Oprl1	−2.3	Mm.285075
Slow skeletal troponin T1	Tnnt1	−3.2	Mm.358643
Wingless-related MMTV integration site 5A	Wnt5a	−2.6	Mm.287544

[a] E16.5 vs E13.5.

(Sox2). Similar expression of Gapdh was used as control. Together, these data demonstrate that the calcineurin/NFAT signaling plays a critical role in transcription induction during myocardium transition. In addition, these data demonstrate a dosage-dependent threshold regulation of the calcineurin/NFAT targets.

Expression of components of calcineurin/NFAT signaling pathway during myocardium transition

Dosage-dependent threshold regulation of the calcineurin/NFAT signaling pathway may, in part, be due to changes in the expression level of calcineurin phosphatases [calcineurin phosphatase catalytic subunit Aα and Aβ (CnAα, and CnAβ), and calcineurin regulatory subunit B (CnB)], NFAT members (NFATc1–c4), and endogenous calcineurin inhibitors Cabin and calcipressin (Csp1–3) (Ryeom et al., 2003), also known as modulatory calcineurin-interacting protein (MCIP) or Down syndrome critical region (DSCR) (Kingsbury and Cunningham, 2000; Rothermel et al., 2000; Rothermel et al., 2003; Vega et al., 2003). RT-PCR analysis demonstrated that the expression of CnAα, CnAβ, and CnB were similar at E13.5 and E16.5 hearts (Fig. 7). Their expression level was not affected by CsA inhibition. Similarly, the expression level of calcineurin inhibitor Cabin and calcipressin (Csp 1–3) was similar. The expression level of NFAT members (NFATc1–c4) was also similar, except NFATc2 exhibited potential alternative spliced isoforms at E13.5. These data demonstrate that the expression of components of the calcineurin/NFAT signaling pathway is similar during myocardium transition. Alterations in intracellular calcium and subsequent activation of the calcineurin/NFAT signaling pathway is likely to account for the threshold regulation.

Formation of NFAT:DNA complex of the Agtr2 and Reg3γ gene

Transcription targets identified by using microarray analysis could be regulated directly or indirectly by the calcineurin/NFAT signaling. NFAT may directly bind to the identified targets and modulate gene transcription. Previous studies indicated that the canonical NFAT element from the interleukin-2 (IL-2) gene is a composite enhancer containing NFAT and AP-1 (Fos and Jun) (Jain et al., 1992). On the other hand, C/EBP is present in the proximal NFAT site of the peroxisome proliferator-activated receptor-γ2 (PPARγ2) gene (Yang and Chow, 2003). Sequence analysis indicated that there are three putative NFAT binding sites (GGAAA) in the Agtr2 promoter (Fig. 8A). These NFAT binding sites are located at −701, −1951, and −5251 bp upstream of the Agtr2 promoter. However, little similarity was found in the adjacent sequence for NFAT partners (AP1 or C/EBP) (Fig. 8B). These observations indicate that Agtr2, a dosage-dependent regulated NFAT target, may be directly regulated by NFAT with partners other than AP1 or C/EBP.

We performed gel mobility shift assays to investigate the formation of NFAT:DNA complex of the Agtr2 NFAT binding elements (Fig. 8C). All three NFAT binding elements of the Agtr2 gene formed NFAT:DNA complexes, indicating that NFAT directly regulates Agtr2 gene. Specificity of the NFAT:DNA complexes was confirmed by supershift analysis using antibody against NFAT and competition analysis using excess amount of unlabeled canonical NFAT site from the IL-2 gene. Interestingly, the Agtr2 NFAT:DNA complex exhibited increased electrophoretic mobility as compared to the IL-2 NFAT:DNA complex. Electrophoretic mobility of NFAT:DNA complex similar to the one found in the Agtr2 gene was also detected using the NFAT binding elements from the Reg3γ gene, another dosage-dependent regulated NFAT target containing NFAT binding elements at −201 and −251 bp upstream of the promoter (Fig. 8). Together, these data indicate that NFAT directly regulates Agtr2 and Reg3γ gene.

The NFAT sites at −701 bp and −1951 bp of the Agtr2 gene and −251 bp of the Reg3γ exhibited increased formation of NFAT:DNA complex (Fig. 8C). Increased intensity suggest formation of a more stable NFAT:DNA complex, which may in part due to abundance of NFAT partners or increased affinity in protein–protein/protein–DNA interactions between NFAT, NFAT partner, and DNA. Next, we investigated the relative binding of different NFAT sites from the IL-2, PPARγ2, Agtr2, and Reg3γ gene by saturation analysis (Fig. 8D). NFAT binding sites from the IL-2 and PPARγ2 gene were selected for comparison because their NFAT partners (AP1 and C/EBP) were both b-ZIP type transcription factors (Jain et al., 1992; Yang and Chow, 2003). Scatchard analysis indicated the relative binding avidity in the NFAT:DNA complex from the Agtr2 and Reg3γ NFAT sites was decreased as compared to the NFAT:AP1 of IL-2 gene and the NFAT:C/EBP of PPARγ2 gene (Fig. 8D). These data indicate that changes in relative binding avidity cannot account for the increased NFAT:DNA complex formation in the Agtr2 and Reg3γ NFAT sites.

Table 3
Transciption targets during myocardium transition—calcineurin/NFAT-dependent

Gene title	Gene symbol	Fold Δ			Unigene ID
E13.5–E16.5 transition, CsA dependent up-regulated genes					
Angiotensin I converting enzyme 2	Ace2	55.0[a]	1.7[b]	1.7[c]	Mm.13451
Carboxylesterase 3	Ces2	27.8	5.6	2.0	Mm.292803
Coronin, actin binding protein 1A	Coro1a	7.0	7.5	9.2	Mm.290482
Deltex 1 homolog	Dtx1	3.7	2.8	2.1	Mm.1645
Keratin complex 2, basic gene 8	Krt2-8	7.0	6.1	8.6	Mm.358618
Lymphoid enhancer binding factor 1	Lef1	2.6	4.3	9.2	Mm.255219
NADPH dehydrogenase quinone 1	Nqo1	2.8	2.0	2.0	Mm.252
Secretoglobin family 1A, member 1	Scgb1a1	48.5	8.0	90.5	Mm.2258
Secretoglobin family 3A, member 1	Scgb3a1	14.9	5.7	11.3	Mm.22802
Transcription factor 7	Tcf7	11.3	16.0	16.0	Mm.31630
Transformation related protein 63	Trp63	7.0	16.0	4.0	Mm.20894
E13.5–E16.5 transition, CsA threshold up-regulated genes					
Angiotensin II receptor type 2	Agtr2	24.3	1.1	5.7	Mm.2679
Carbonyl reductase 2	Cbr2	36.7	2.8	45.2	Mm.21454
Cytochrome P450 Family 2, subfamily f, polypeptide 2	Cyp2f2	45.3	2.1	42.2	Mm.4515
Forkhead box A1	Foxa1	8.0	2.5	68.6	Mm.4578
Regenerating islet-derived 3 gamma	Reg3g	111.4	3.5	42.2	Mm.252385
SRY-box containing gene 2	Sox2	3.7	2.6	36.7	Mm.4541
E13.5–E16.5 transition independent, CsA dependent up-regulated genes					
Lymphocyte cytosolic protein 1	Lcp1	ND	2.1	2.1	Mm.153911
Ras association domain family 5	Rassf5	ND	2.1	1.9	Mm.248291

[a] E16.5 vs E13.5.
[b] E16.5: Untreated vs Lo CsA.
[c] E16.5: Untreated vs Hi CsA.

To confirm the NFAT:DNA complex from the Agtr2 and Reg3γ NFAT sites exhibit reduced binding avidity, we performed cross competition analysis (Fig. 8E). Formation of NFAT:DNA complex by the IL-2 NFAT site was reduced by self competition using unlabeled oligonucleotides. At five times excess of competitors in self competition, ~10% NFAT:DNA complex remained bound to the IL-2 NFAT:AP1 site. At 10 times excess of competitors in self competition, formation of NFAT:DNA complex on the IL-2 NFAT:AP1 site was hardly detected. At least ~50% of IL-2 NFAT:DNA complex, however, remained bound even in the presence of 25 times excess of unlabeled Agtr2 or Reg3γ NFAT sites as competitors. Conversely, the amount of NFAT:DNA complex formed by the Agtr2 or Reg3γ NFAT probes was competed to a similar extent by the IL-2 NFAT sites or by self competition. These data confirm that the relative binding avidity from the Agtr2 and Reg3γ NFAT sites is reduced as compared to the NFAT:AP1 site of the IL-2 gene. Together, the increase in electrophoretic mobility and the difference in relative binding avidity indicate that formation of distinct NFAT:DNA complexes, in part, accounts for the dosage-dependent regulation mediated by the calcineurin/NFAT signaling.

Discussion

Molecular targets in E13.5–E16.5 myocardium transition

In this report, we have profiled transcription targets during E13.5–E16.5 myocardium transition. Coupling with calcineurin specific inhibitor — cyclosporin A (CsA), we have further identified genes regulated dependently and independently by the calcineurin/NFAT signaling pathway. Our results demonstrated that about a-third of the induced genes during E13.5–E16.5 myocardium transition is regulated by the calcineurin/NFAT signaling pathway. Among the calcineurin/NFAT regulated genes, there is a dosage-dependent regulation of their expression. Dosage-dependent calcineurin/NFAT inhibition is also revealed by a graded disruption in heart morphogenesis. Together, these results demonstrate a critical role for the calcineurin/NFAT signaling pathway in heart development.

Among the calcineurin/NFAT targets, structural genes [*e.g.* coronin, actin binding protein 1A (Coro1a), and keratin complex 2, basic gene 8 (Krt2-8)] and molecular targets involved in mitochondrial biogenesis [*e.g.* carboxylesterase 3 (Ces3), NADPH dehydrogenase quinone 1 (Nqo1), carbonyl reductase 2 (Cbr2), and cytochrome P450 family 2, subfamily f, polypeptide 2 (Cyp2f2)] are identified. Identification of these structural genes and mitochondrial targets support the role of NFAT in cellular architecture and redox regulation (Bushdid et al., 2003).

In addition to the structural genes and mitochondrial targets, secretory factors, such as members of the secretoglobin (Scgb) family, are revealed in this study. Members of the secretoglobin family are critical for regulation of lung function (Cassel et al., 2002; Reynolds et al., 2002). Interestingly, lung morphogenesis takes place after heart formation (Kaufman, 1992; Kaufman and Bard, 1999). The expression of Scgb proteins in embryonic heart and their functions in lung morphogenesis suggest a

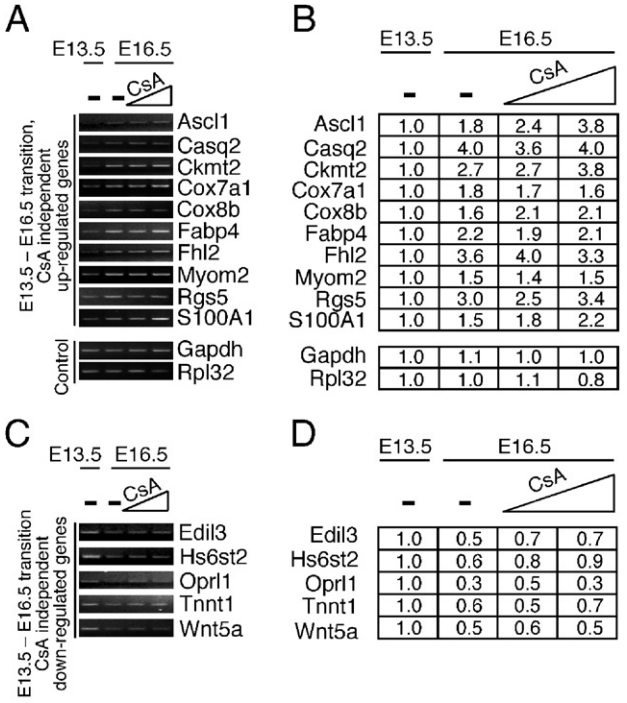

Fig. 4. Calcineurin/NFAT-independent transcription regulation during myocardium transition. A–B) RT-PCR analysis to illustrate transcription targets that were increased, but calcineurin/NFAT-independent, during E13.5 to E16.5 myocardium transition (panel A). Two different dosages of CsA were used to probe the requirement of calcineurin/NFAT during myocardium transition. Expression of Gapdh (glyceraldehydes-3-phosphate dehydrogenase) and Rpl32 (ribosomal protein L32) were used as controls. Quantification of PCR products using ImageQuant software was also shown (panel B). Ascl1, Acyl-CoA synthetase long-chain family member 1; Casq2, Calsequestrin 2; Ckmt2, Creatine kinase mitochondrial 2; Cox7a1, Cytochrome *c* oxidase subunit VIIa1; Cox8b, Cytochrome *c* oxidase subunit VIIIb; Fabp4, Fatty acid binding protein 4; Fhl2, Four and a half LIM domains 2; Myom2, Myomesin 2; Rgs5, Regulator of G-protein signaling 5; and S00A1, S100 calcium binding protein A1. C–D) RT-PCR analysis to illustrate transcripton targets that were decreased, but calcineurin/NFAT-independent, during E13.5 to E16.5 myocardium transition (panel C). Quantification of PCR products using ImageQuant software was also shown (panel D). Edil3, EGF-like repeats and discoidin I-like domain 3; Hs6st2, Heparin sulfate 6-*O*-sulfotransferase 2; Oprl1, Opioid receptor-like 1; Tnnt1, Slow skeletal troponin T1; and Wnt5a, Wingless-related MMTV integration site 5A.

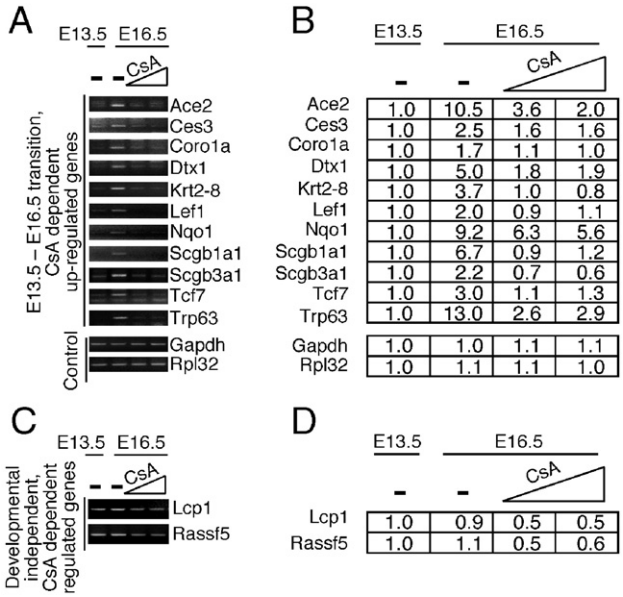

Fig. 5. Transcription targets regulated by the calcineurin/NFAT signaling during myocardium transition. A–B) RT-PCR analysis to illustrate calcineurin/NFAT-dependent transcription targets that were increased during E13.5 to E16.5 myocardium transition (panel A). Two different dosages of CsA were used to probe the requirement of calcineurin/NFAT during myocardium transition. Expression of Gapdh (glyceraldehydes-3-phosphate dehydrogenase) and Rpl32 (ribosomal protein L32) were used as controls. Quantification of PCR products using ImageQuant software was also shown (panel B). Ace2, Angiotensin I converting enzyme 2; Ces3, Carboxylesterase 3; Coro1a, Coronin, actin binding protein 1A; Dtx1, Deltex 1 homolog; Krt2-8, Keratin complex 2, basic gene 8; Lef1, Lymphoid enhancer binding factor 1; Nqo1, NADPH dehydrogenase quinone 1; Scgb1a1, Secretoglobin family 1A, member 1; Scgb3a1, Secretoglobin family 3A, member 1; Tcf7, Transcription factor 7; and Trp63, Transformation related protein 63. C–D) RT-PCR analysis to illustrate transcription targets that were sensitive to CsA inhibition, but are not regulated upon E13.5–E16.5 myocardium transition (panel C). Quantification of PCR products using ImageQuant software was also shown (panel D). Lcp1, Lymphocyte cytosolic protein 1; Rassf5, Ras association domain family 5.

possible endocrine relationship through the pulmonary circuitry during development.

Regenerating islet-derived 3 gamma (Reg3γ), another secretory factor, is regulated by the calcineurin/NFAT signaling pathway in a threshold-dependent manner. Requirement of high inhibition to block Reg3γ expression suggests that a minimal calcineurin/NFAT activity is sufficient for the transcription induction during myocardium transition. This minimal requirement implicates that Reg3γ is critical for myocardium transition. Members of the Reg family were identified as critical mitogens for regeneration/proliferation in various tissues (Okamoto, 1999; Terazono et al., 1988). Myocardium transition, similar to regeneration, requires mitogenic factors to stimulate proliferation and remodeling. Since diseased heart exhibits characteristics of embryonic heart and reactivates fetal gene program, and the calcineurin/NFAT signaling pathway is

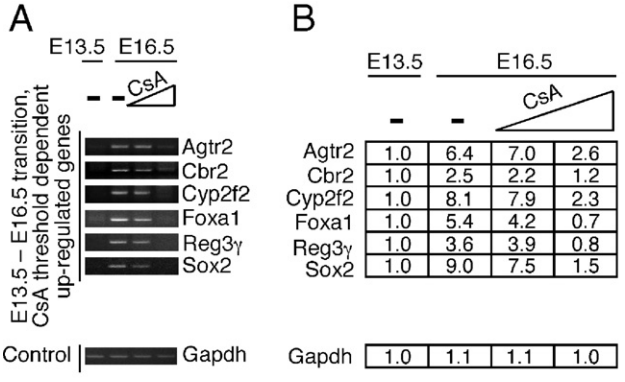

Fig. 6. Dosage-dependent threshold requirement on transcription targets regulated by the calcineurin/NFAT signaling during myocardium transition. A–B) RT-PCR analysis to illustrate transcription targets that were only sensitive to high dosage of CsA inhibition during E13.5–E16.5 myocardium transition (panel A). Expression of Gapdh (glyceraldehydes-3-phosphate dehydrogenase) was used as a control. Quantification of PCR products using ImageQuant software was also shown (panel B). Agtr2, Angiotensin II receptor type 2; Cbr2, Carbonyl reductase 2; Cyp2f2, Cytochrome P450 Family 2, subfamily f, polypeptide 2; Foxa1, Forkhead box A1; Reg3γ, Regenerating islet-derived 3 gamma; and Sox2, SRY-box containing gene 2.

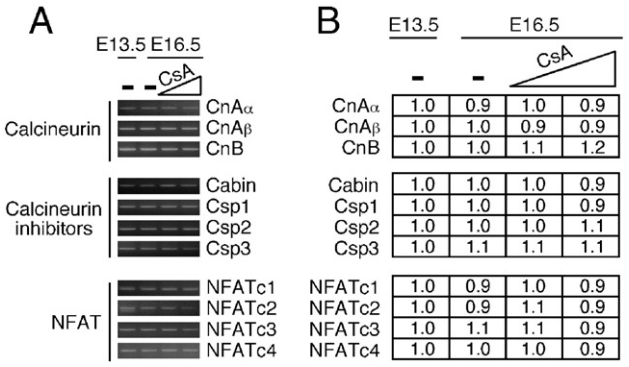

Fig. 7. Expression of components of the calcineurin/NFAT signaling pathway during myocardium transition. A–B) RT-PCR analysis to examine the expression level of components of the calcineurin/NFAT signaling pathway during E13.5 to E16.5 myocardium transition (panel A). CsA-treated hearts were also examined. Quantification of PCR products using ImageQuant software was also shown (panel B). CnAα, calcineurin phosphatase catalytic subunit Aα; CnAβ, calcineurin phosphatase catalytic subunit Aβ; CnB, calcineurin regulatory subunit B; Csp, calcipressin.

critical for heart function, it is tempting to speculate that Reg members may be up-regulated for possible heart "regeneration" after insult. Thus, cardiomyocytes expressing Reg mitogen may be molecular markers for characterizing potential multipotent cells in heart during recovery, in addition to its potential role during myocardium transition. A goal for future studies is to elucidate the role of Reg members in cardiac stem cells and in heart development.

In addition, dosage-dependent regulation of the expression of angiotensin II receptor type 2 (Agtr2) is of interest. Agtr2 is expressed mainly in developing myocardium and hypertrophic heart (Grady et al., 1991; Wang et al., 1998). Similar to Reg3γ, minimal Agtr2 expression is detected after birth and in normal adult heart. Previous studies demonstrated that transgenic mice expressing Agtr2 in heart leaded to dosage-dependent cardiomyopathy and dysregulation in heart function (Nakayama et al., 2005; Yan et al., 2003). Hence, the extent of NFAT activation and its subsequent gene transcription may directly correlate with heart function.

Here, we have demonstrated that the calcineurin/NFAT signaling pathway regulates the expression of one-third of the induced genes during myocardium transition. Transcription regulation of the remaining two-third, however, remains to be identified. Signaling pathways that may involve in the transcription regulation of the remaining two-third of genes may include the G-protein coupled receptor (GPCR) pathway, TGFβ/BMP signal transduction, and Tyr receptor kinase signaling (Brand and Schneider, 1995; Negro et al., 2004; Rockman et al., 2002; Wetzker and Rommel, 2004). Certain targets during myocardium transition may also be co-regulated by different signaling pathways. Contribution of these additional pathways in modulating myocardium transition may be assessed by similar reductionist approach using specific inhibitors in microarray analysis to identify differentially expressed targets.

Dosage-dependent threshold regulation of the calcineurin/NFAT-mediated gene transcription

The calcineurin/NFAT signaling pathway was first characterized in immune models (Crabtree and Olson, 2002; Hogan et al., 2003; Horsley and Pavlath, 2002; Macian, 2005). Subsequent studies have extended the calcineurin/NFAT regulation and function to non-immune cells. In this report, we have demonstrated that a dosage-dependent requirement plays a role in calcineurin/NFAT-mediated gene transcription during myocardium transition. Mechanistically, formation of distinct NFAT:DNA complexes, in part, accounts for the differential regulation. Similar dosage-dependent requirement for the calcineurin/NFAT signaling pathway has been reported in regulating immune function (Ryeom et al., 2003). Hence, dosage-dependent regulation provides another means for modulating calcineurin/NFAT-mediated gene transcription.

Transcription factor NFAT constantly shuttles between nucleus and cytoplasm (Kehlenbach et al., 1998; Shibasaki et al., 1996). Continuous shuttling between the nuclear and cytoplasmic compartment may provide a "partial" activation state and allow subsequent transcription of the dosage-sensitive target genes. Upon elevation in intracellular calcium, calcineurin-mediated dephosphorylation favors NFAT nuclear import. Dephosphorylation, which is illustrated by substantial increase in electrophoretic mobility, has been served as a hallmark for NFAT activation (Chow et al., 1997; Loh et al., 1996; Yang et al., 2002). If transcription of dosage-sensitive targets only requires minimal calcineurin/NFAT activity, the basal, transiently resided nuclear NFAT in resting cells would be sufficient for their expression. Hence, complete dephosphorylation and the substantial increase in electrophoretic mobility may not be required for certain NFAT-mediated gene transcription.

Fig. 8. Formation of NFAT:DNA complex of the Agtr2 and Reg3γ gene. A) Schematic illustration of the Agtr2 and the Reg3γ promoter. NFAT binding elements were indicated by filled triangles. B) Sequence comparison of the NFAT binding sites in IL-2, PPARγ2, Reg3γ and Agtr2 gene promoters. Canonical NFAT-binding site is illustrated (filled box). Adjacent NFAT partner binding site was also indicated (AP-1, shaded box; C/EBP, hatched box). Residues on the Reg3γ and Agtr2 NFAT sites that resemble the AP-1 (*) or C/EBP (^) binding sequence were also indicated. C) Formation of distinct NFAT complexes on the Reg3γ and Agtr2-binding elements. NFAT:DNA complexes (open triangles) from IL-2, Reg3γ, and Agtr2 NFAT sites were supershifted with antibody against NFAT (asterisks). NFAT:DNA complexes were competed by excess amounts of unlabeled canonical NFAT binding element from the IL-2 gene. D) Saturation analysis to determine the relative binding of different NFAT sites. IL-2 NFAT:AP1 site (open squares on dotted line) and PPARγ2 NFAT:C/EBP site (open circles on dotted line) were used for comparison to the Agtr2 NFAT sites (at −701 bp: filled squares on solid line; at −1951 bp: filled triangles on solid line), and Reg3γ −251 bp NFAT site (filled circles on solid line). Average linear correlation coefficient of each probe in the data set is ≥0.94. Slope of the graph represents relative binding avidity of different NFAT probes and presented. Amount of bound NFAT:DNA complex and free DNA probe was quantitated by PhosphoImager analysis. The ratio of bound/free was plotted against the amount of bound and graphed. E) Cross-competition analysis to assess NFAT DNA binding in IL-2, Agtr2, and Reg3γ NFAT sites. Increasing amount of unlabeled NFAT binding elements as competitors (500, 1000, 2500 fmol) were incubated with the indicated probe. Formation of NFAT:DNA complex was visualized by autoradiography.

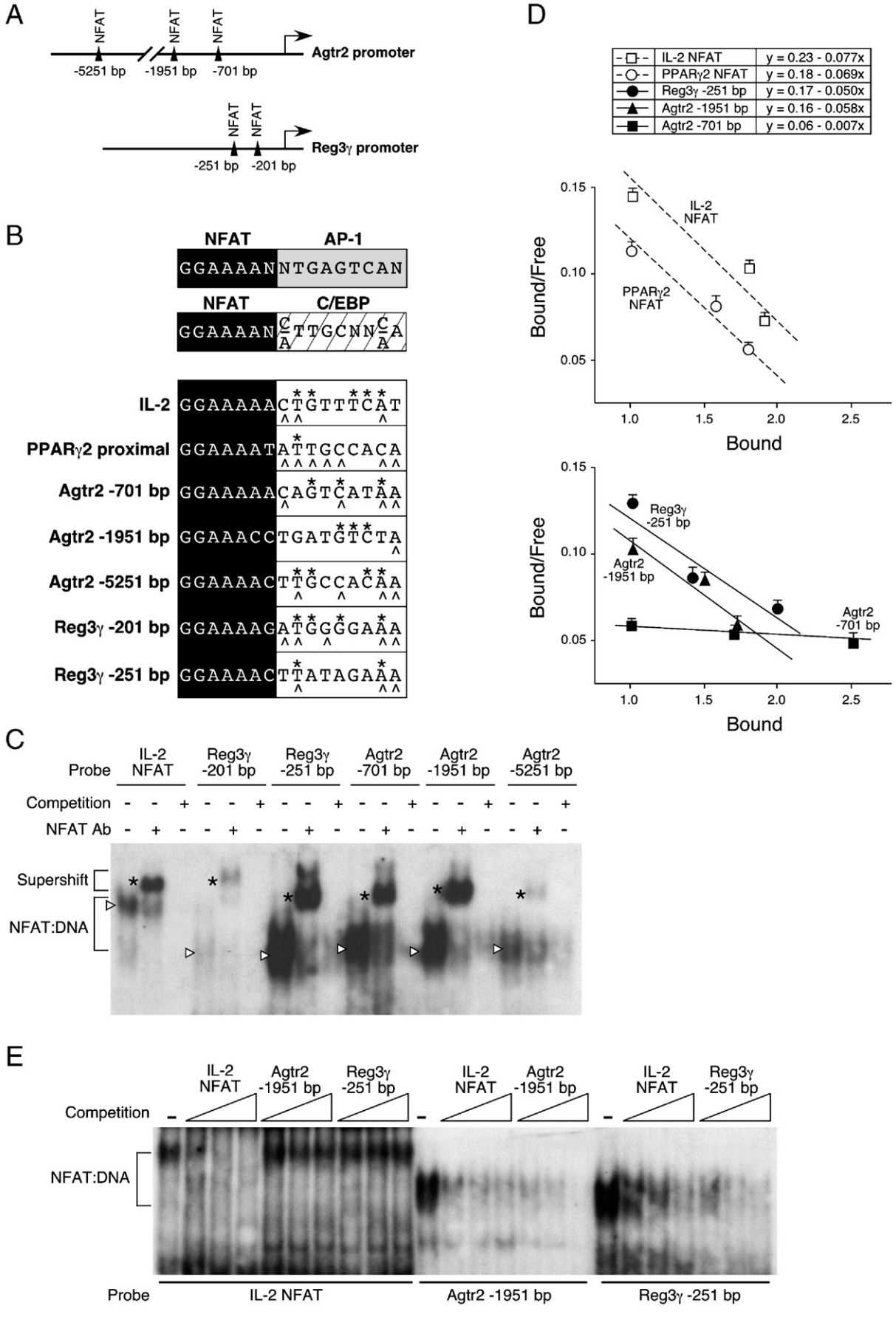
A
NFAT
NFAT
NFAT
-5251 bp
-1951 bp
-701 bp
Agtr2 promoter
NFAT
NFAT
-251 bp
-201 bp
Reg3γ promoter
B
NFAT
AP-1
GGAAAANNTGAGTCAN
NFAT
C/EBP
GGAAAAN
TTGCNN
IL-2 GGAAAAACTGTTTCAT
PPARγ2 proximal GGAAAATATTGCCACA
Agtr2 -701 bp GGAAAAACAGTCATAA
Agtr2 -1951 bp GGAAACCTGATGTCTA
Agtr2 -5251 bp GGAAAACTTGCCACAA
Reg3γ -201 bp GGAAAAGATGGGGAAA
Reg3γ -251 bp GGAAAACTTATAGAAA
D
IL-2 NFAT y = 0.23 - 0.077x
PPARγ2 NFAT y = 0.18 - 0.069x
Reg3γ -251 bp y = 0.17 - 0.050x
Agtr2 -1951 bp y = 0.16 - 0.058x
Agtr2 -701 bp y = 0.06 - 0.007x
Bound/Free
0.15
0.10
0.05
IL-2 NFAT
PPARγ2 NFAT
1.0
1.5
2.0
2.5
Bound
Reg3γ -251 bp
Agtr2 -1951 bp
Agtr2 -701 bp
C
Probe
IL-2 NFAT
Reg3γ -201 bp
Reg3γ -251 bp
Agtr2 -701 bp
Agtr2 -1951 bp
Agtr2 -5251 bp
Competition
NFAT Ab
Supershift
NFAT:DNA
E
IL-2 NFAT
Agtr2 -1951 bp
Reg3γ -251 bp
Competition
NFAT:DNA
Probe
IL-2 NFAT
Agtr2 -1951 bp
Reg3γ -251 bp

Once NFAT is resided in the nucleus, NFAT interacts with NFAT partners to form a composite binding elements for gene regulation. For example, AP-1 (Fos+Jun) are NFAT partners on the IL-2 gene (Jain et al., 1992). The NFAT:DNA complexes from the Agtr2 and the Reg3γ gene exhibit increased electrophoretic mobility as compared to that from the IL-2 gene, suggesting that partners other than AP-1 cooperate with NFAT to regulate gene expression. Since the NFAT:DNA complexes are separated by non-denaturing gel electrophoresis, the partners of Agtr2 and Reg3γ gene may be lower in molecular weight or enriched in acidic amino acid residues. Alternatively, a more compact ordered arrangement may be found in the NFAT:DNA complexes of the Agtr2 and the Reg3γ gene.

In addition to the increase in electrophoretic mobility, certain NFAT:DNA complexes from the Agtr2 (Agtr2 −701 bp and −1951 bp) and the Reg3γ (Reg3γ −251 bp) gene exhibit increase in intensity as compared to that from the IL-2 gene. Increased intensity suggest formation of a more stable NFAT:DNA complex, which may in part due to the abundance of NFAT partners or increased affinity in protein–protein/protein–DNA interactions between NFAT, NFAT partner, and DNA. Since the Agtr2 and Reg3γ NFAT sites exhibit reduced relative binding avidity as compared to the IL-2 NFAT:AP1 site, it is likely that the abundance of partners for the Agtr2 and Reg3γ NFAT sites accounts for the increased formation of NFAT:DNA complex. Binding of different partners exerts another layer of regulation on NFAT-mediated gene transcription. Hence, activation of dosage-dependent regulated genes is possibly due to efficient cooperation between NFAT and its highly expressed partners. Identification of such NFAT partners is an immediate goal to further elucidate regulation of NFAT-mediated gene transcription in heart function.

We have demonstrated that the expression levels of components of the calcineurin/NFAT signaling pathway are similar during myocardium transition. These components include calcineurin phosphatases (CnAα, CnAβ, CnB), calcineurin inhibitors (Cabin, and Csp1–3), and NFAT (NFATc1–c4). We surmise that alterations in intracellular calcium and subsequent activation of the calcineurin/NFAT signaling pathway are likely to account for the dosage-dependent regulation. A recent report, indeed, indicated that a 1.5 fold change in the expression of a NFAT kinase – Dyrk1a – may be sufficient to cause Down's syndrome (Arron et al., 2006). Dyrk1a kinase opposes the accumulation of nuclear NFAT (Arron et al., 2006; Gwack et al., 2006). Hence, the duration in the nucleus is a critical parameter for the dosage-dependent threshold regulation mediated by NFAT.

In addition to NFAT, many other transcription factors are also regulated by nuclear/cytoplasmic shuttling mechanism (Cartwright and Helin, 2000; Smith and Koopman, 2004). Their "partial/transient" localization in the nucleus may be sufficient to modulate gene transcription in a dosage-dependent manner. Since minimal basal activity is sufficient for the expression of these dosage-sensitive targets, these genes are likely to be the rate-limiting components or essential genes. Further identification and characterization of these threshold-sensitive targets are warranted.

Conclusion

In conclusion, we have demonstrated that the calcineurin/NFAT signaling contributes to the expression of one-third of genes during the E13.5–E16.5 myocardium transition. Expression of the calcineurin/NFAT-dependent transcription target is, in part, regulated by a dosage-dependent threshold mechanism. Thus, in addition to temporal and spatial control, dosage-dependent regulation provides another mechanism to modulate transcriptional response mediated by the calcineurin/NFAT signaling.

Acknowledgments

We thank members of our laboratories for their critical reading of the manuscript. This research is supported, in part, by a grant from the American Heart Association.

Appendix A. Supplementary data

Supplementary data associated with this article can be found, in the online version, at doi:10.1016/j.ydbio.2006.11.036.

References

Arron, J.R., Winslow, M.M., Polleri, A., Chang, C.P., Wu, H., Gao, X., Neilson, J.R., Chen, L., Heit, J.J., Kim, S.K., Yamasaki, N., Miyakawa, T., Francke, U., Graef, I.A., Crabtree, G.R., 2006. NFAT dysregulation by increased dosage of DSCR1 and DYRK1A on chromosome 21. Nature 441, 595–600.

Brand, T., Schneider, M.D., 1995. The TGF beta superfamily in myocardium: ligands, receptors, transduction, and function. J. Mol. Cell. Cardiol. 27, 5–18.

Bruneau, B.G., 2002. Transcriptional regulation of vertebrate cardiac morphogenesis. Circ. Res. 90, 509–519.

Bueno, O.F., van Rooij, E., Molkentin, J.D., Doevendans, P.A., De Windt, L.J., 2002. Calcineurin and hypertrophic heart disease: novel insights and remaining questions. Cardiovasc. Res. 53, 806–821.

Bushdid, P.B., Osinska, H., Waclaw, R.R., Molkentin, J.D., Yutzey, K.E., 2003. NFATc3 and NFATc4 are required for cardiac development and mitochondrial function. Circ. Res. 92, 1305–1313.

Cartwright, P., Helin, K., 2000. Nucleocytoplasmic shuttling of transcription factors. Cell. Mol. Life Sci. 57, 1193–1206.

Cassel, T.N., Berg, T., Suske, G., Nord, M., 2002. Synergistic transactivation of the differentiation-dependent lung gene Clara cell secretory protein (secretoglobin 1a1) by the basic region leucine zipper factor CCAAT/enhancer-binding protein alpha and the homeodomain factor Nkx2.1/thyroid transcription factor-1. J. Biol. Chem. 277, 36970–36977.

Chang, C.P., Neilson, J.R., Bayle, J.H., Gestwicki, J.E., Kuo, A., Stankunas, K., Graef, I.A., Crabtree, G.R., 2004. A field of myocardial–endocardial NFAT signaling underlies heart valve morphogenesis. Cell 118, 649–663.

Chow, C.W., Rincon, M., Cavanagh, J., Dickens, M., Davis, R.J., 1997. Nuclear accumulation of NFAT4 opposed by the JNK signal transduction pathway. Science 278, 1638–1641.

Crabtree, G.R., Olson, E.N., 2002. NFAT signaling: choreographing the social lives of cells. Cell 109, S67–S79 (Suppl.).

de la Pompa, J.L., Timmerman, L.A., Takimoto, H., Yoshida, H., Elia, A.J., Samper, E., Potter, J., Wakeham, A., Marengere, L., Langille, B.L., Crabtree, G.R., Mak, T.W., 1998. Role of the NF-ATc transcription factor in morphogenesis of cardiac valves and septum. Nature 392, 182–186.

Frey, N., Olson, E.N., 2003. Cardiac hypertrophy: the good, the bad, and the ugly. Annu. Rev. Physiol. 65, 45–79.

Gafter-Gvili, A., Sredni, B., Gal, R., Gafter, U., Kalechman, Y., 2003.

Cyclosporin A-induced hair growth in mice is associated with inhibition of calcineurin-dependent activation of NFAT in follicular keratinocytes. Am. J. Physiol.: Cell Physiol. 284, C1593–C1603.
Grady, E.F., Sechi, L.A., Griffin, C.A., Schambelan, M., Kalinyak, J.E., 1991. Expression of AT2 receptors in the developing rat fetus. J. Clin. Invest. 88, 921–933.
Graef, I.A., Chen, F., Chen, L., Kuo, A., Crabtree, G.R., 2001. Signals transduced by Ca2+/calcineurin and NFATc3/c4 pattern the developing vasculature. Cell 105, 863–875.
Gwack, Y., Sharma, S., Nardone, J., Tanasa, B., Iuga, A., Srikanth, S., Okamura, H., Bolton, D., Feske, S., Hogan, P.G., Rao, A., 2006. A genome-wide Drosophila RNAi screen identifies DYRK-family kinases as regulators of NFAT. Nature 441, 646–650.
Harvey, R.P., Rosenthal, N., 1999. Heart Development. Academic Press, San Diego.
Hogan, P.G., Chen, L., Nardone, J., Rao, A., 2003. Transcriptional regulation by calcium, calcineurin, and NFAT. Genes Dev. 17, 2205–2232.
Horsley, V., Pavlath, G.K., 2002. Nfat: ubiquitous regulator of cell differentiation and adaptation. J. Cell Biol. 156, 771–774.
Jain, J., McCaffrey, P.G., Valge-Archer, V.E., Rao, A., 1992. Nuclear factor of activated T cells contains Fos and Jun. Nature 356, 801–804.
Kaufman, M.H., 1992. The Atlas of Mouse Development. Academic Press, London; San Diego.
Kaufman, M.H., Bard, J.B.L., 1999. The Anatomical Basis of Mouse Development. Academic Press, San Diego.
Kehlenbach, R.H., Dickmanns, A., Gerace, L., 1998. Nucleocytoplasmic shuttling factors including Ran and CRM1 mediate nuclear export of NFAT In vitro. J. Cell Biol. 141, 863–874.
Kingsbury, T.J., Cunningham, K.W., 2000. A conserved family of calcineurin regulators. Genes Dev. 14, 1595–1604.
Loh, C., Shaw, K.T., Carew, J., Viola, J.P., Luo, C., Perrino, B.A., Rao, A., 1996. Calcineurin binds the transcription factor NFAT1 and reversibly regulates its activity. J. Biol. Chem. 271, 10884–10891.
Macian, F., 2005. NFAT proteins: key regulators of T-cell development and function. Nat. Rev., Immunol. 5, 472–484.
MacLellan, W.R., Schneider, M.D., 2000. Genetic dissection of cardiac growth control pathways. Annu. Rev. Physiol. 62, 289–319.
Molkentin, J.D., Dorn II, I.G., 2001. Cytoplasmic signaling pathways that regulate cardiac hypertrophy. Annu. Rev. Physiol. 63, 391–426.
Molkentin, J.D., Lu, J.R., Antos, C.L., Markham, B., Richardson, J., Robbins, J., Grant, S.R., Olson, E.N., 1998. A calcineurin-dependent transcriptional pathway for cardiac hypertrophy. Cell 93, 215–228.
Nakayama, M., Yan, X., Price, R.L., Borg, T.K., Ito, K., Sanbe, A., Robbins, J., Lorell, B.H., 2005. Chronic ventricular myocyte-specific overexpression of angiotensin II type 2 receptor results in intrinsic myocyte contractile dysfunction. Am. J. Physiol.: Heart Circ. Physiol. 288, H317–H327.
Negro, A., Brar, B.K., Lee, K.F., 2004. Essential roles of Her2/erbB2 in cardiac development and function. Recent Prog. Horm. Res. 59, 1–12.
Okamoto, H., 1999. The Reg gene family and Reg proteins: with special attention to the regeneration of pancreatic beta-cells. J. Hepatobiliary Pancreat. Surg. 6, 254–262.
Petrich, B.G., Wang, Y., 2004. Stress-activated MAP kinases in cardiac remodeling and heart failure; new insights from transgenic studies. Trends Cardiovasc. Med. 14, 50–55.
Ranger, A.M., Grusby, M.J., Hodge, M.R., Gravallese, E.M., de la Brousse, F.C., Hoey, T., Mickanin, C., Baldwin, H.S., Glimcher, L.H., 1998. The transcription factor NF-ATc is essential for cardiac valve formation. Nature 392, 186–190.
Reynolds, S.D., Reynolds, P.R., Pryhuber, G.S., Finder, J.D., Stripp, B.R., 2002. Secretoglobins SCGB3A1 and SCGB3A2 define secretory cell subsets in mouse and human airways. Am. J. Respir. Crit. Care Med. 166, 1498–1509.
Rockman, H.A., Koch, W.J., Lefkowitz, R.J., 2002. Seven-transmembrane-spanning receptors and heart function. Nature 415, 206–212.
Rothermel, B., Vega, R.B., Yang, J., Wu, H., Bassel-Duby, R., Williams, R.S., 2000. A protein encoded within the Down syndrome critical region is enriched in striated muscles and inhibits calcineurin signaling. J. Biol. Chem. 275, 8719–8725.
Rothermel, B.A., Vega, R.B., Williams, R.S., 2003. The role of modulatory calcineurin-interacting proteins in calcineurin signaling. Trends Cardiovasc. Med. 13, 15–21.
Ryeom, S., Greenwald, R.J., Sharpe, A.H., McKeon, F., 2003. The threshold pattern of calcineurin-dependent gene expression is altered by loss of the endogenous inhibitor calcipressin. Nat. Immunol. 4, 874–881.
Schubert, W., Yang, X.Y., Yang, T.T., Factor, S.M., Lisanti, M.P., Molkentin, J.D., Rincon, M., Chow, C.W., 2003. Requirement of transcription factor NFAT in developing atrial myocardium. J. Cell Biol. 161, 861–874.
Shibasaki, F., Price, E.R., Milan, D., McKeon, F., 1996. Role of kinases and the phosphatase calcineurin in the nuclear shuttling of transcription factor NF-AT4. Nature 382, 370–373.
Smith, J.M., Koopman, P.A., 2004. The ins and outs of transcriptional control: nucleocytoplasmic shuttling in development and disease. Trends Genet. 20, 4–8.
Srivastava, D., 2001. Genetic assembly of the heart: implications for congenital heart disease. Annu. Rev. Physiol. 63, 451–469.
Srivastava, D., Olson, E.N., 2000. A genetic blueprint for cardiac development. Nature 407, 221–226.
Terazono, K., Yamamoto, H., Takasawa, S., Shiga, K., Yonemura, Y., Tochino, Y., Okamoto, H., 1988. A novel gene activated in regenerating islets. J. Biol. Chem. 263, 2111–2114.
Vega, R.B., Rothermel, B.A., Weinheimer, C.J., Kovacs, A., Naseem, R.H., Bassel-Duby, R., Williams, R.S., Olson, E.N., 2003. Dual roles of modulatory calcineurin-interacting protein 1 in cardiac hypertrophy. Proc. Natl. Acad. Sci. U. S. A. 100, 669–674.
Wang, Z.Q., Moore, A.F., Ozono, R., Siragy, H.M., Carey, R.M., 1998. Immunolocalization of subtype 2 angiotensin II (AT2) receptor protein in rat heart. Hypertension 32, 78–83.
Wetzker, R., Rommel, C., 2004. Phosphoinositide 3-kinases as targets for therapeutic intervention. Curr. Pharm. Des. 10, 1915–1922.
Yan, X., Price, R.L., Nakayama, M., Ito, K., Schuldt, A.J., Manning, W.J., Sanbe, A., Borg, T.K., Robbins, J., Lorell, B.H., 2003. Ventricular-specific expression of angiotensin II type 2 receptors causes dilated cardiomyopathy and heart failure in transgenic mice. Am. J. Physiol.: Heart Circ. Physiol. 285, H2179–H2187.
Yang, T.T., Chow, C.W., 2003. Transcription cooperation by NFAT.C/EBP composite enhancer complex. J. Biol. Chem. 278, 15874–15885.
Yang, T.T., Xiong, Q., Enslen, H., Davis, R.J., Chow, C.W., 2002. Phosphorylation of NFATc4 by p38 mitogen-activated protein kinases. Mol. Cell. Biol. 22, 3892–3904.
Zhang, W., 2002. Old and new tools to dissect calcineurin's role in pressure-overload cardiac hypertrophy. Cardiovasc. Res. 53, 294–303.